



**HAL**  
open science

## Collective Motion of Self-Propelled Particles with Memory

Ken H. Nagai, Yutaka Sumino, Raul Montagne, Igor S. Aranson, Hugues Chaté

► **To cite this version:**

Ken H. Nagai, Yutaka Sumino, Raul Montagne, Igor S. Aranson, Hugues Chaté. Collective Motion of Self-Propelled Particles with Memory. *Physical Review Letters*, 2015, 114, pp.168001. 10.1103/PhysRevLett.114.168001. cea-01367162

**HAL Id: cea-01367162**

**<https://cea.hal.science/cea-01367162>**

Submitted on 15 Sep 2016

**HAL** is a multi-disciplinary open access archive for the deposit and dissemination of scientific research documents, whether they are published or not. The documents may come from teaching and research institutions in France or abroad, or from public or private research centers.

L'archive ouverte pluridisciplinaire **HAL**, est destinée au dépôt et à la diffusion de documents scientifiques de niveau recherche, publiés ou non, émanant des établissements d'enseignement et de recherche français ou étrangers, des laboratoires publics ou privés.



## Collective Motion of Self-Propelled Particles with Memory

Ken H. Nagai,<sup>1</sup> Yutaka Sumino,<sup>2</sup> Raul Montagne,<sup>3</sup> Igor S. Aranson,<sup>4</sup> and Hugues Chaté<sup>5,6,7</sup>

<sup>1</sup>*School of Materials Science, Japan Advanced Institute of Science and Technology, Ishikawa 923-1292, Japan*

<sup>2</sup>*Department of Applied Physics, Tokyo University of Science, Tokyo 125-8585, Japan*

<sup>3</sup>*Departamento de Física, UFRPE, 52171-900 Recife, Pernambuco, Brazil*

<sup>4</sup>*Materials Science Division, Argonne National Laboratory, Argonne, Illinois 60439, USA*

<sup>5</sup>*Service de Physique de l'Etat Condensé, CNRS UMR 3680, CEA-Saclay, 91191 Gif-sur-Yvette, France*

<sup>6</sup>*LPTMC, CNRS UMR 7600, Université Pierre et Marie Curie, 75252 Paris, France*

<sup>7</sup>*Beijing Computational Science Research Center, 3 Heqing Road, Beijing 100080, China*

(Received 30 January 2015; published 24 April 2015)

We show that memory, in the form of underdamped angular dynamics, is a crucial ingredient for the collective properties of self-propelled particles. Using Vicsek-style models with an Ornstein-Uhlenbeck process acting on angular velocity, we uncover a rich variety of collective phases not observed in usual overdamped systems, including vortex lattices and active foams. In a model with strictly nematic interactions the smectic arrangement of Vicsek waves giving rise to global polar order is observed. We also provide a calculation of the effective interaction between vortices in the case where a telegraphic noise process is at play, explaining thus the emergence and structure of the vortex lattices observed here and in motility assay experiments.

DOI: [10.1103/PhysRevLett.114.168001](https://doi.org/10.1103/PhysRevLett.114.168001)

PACS numbers: 45.70.Vn, 05.65.+b, 82.70.Dd, 87.18.Gh

Self-propelled particles are nowadays commonly used to study collective motion and more generally “dry” active matter, where the surrounding fluid is neglected. Real world relevant situations include shaken granular particles [1–5], active colloids [6–8], and biofilaments displaced by motor proteins [9–11]. The trajectories of moving living organisms (from bacteria to large animals such as fish, birds, and even human crowds) are also routinely modeled by such particles, see, e.g., Refs. [12–17].

Many of these “active particles” travel at near-constant speed with their dynamics modeled as a persistent random walk with some stochastic component acting directly on their orientation [18]. This noise, which represents external and/or internal perturbations, produces jagged irregular trajectories. Most of the recent results on active matter have been obtained in this context of overdamped dynamics.

In many situations, however, the overdamped approximation is not justified. In particular, trajectories can be essentially smooth, as for chemically propelled rods [19,20], birds, some large fish that swim steadily [16], or even biofilaments in motility assays with a high density of molecular motors [10]. Whether underdamped dynamics can make a difference at the level of collective asymptotic properties is largely unknown. Interesting related progress was recently reported for starling flocks [21]. Underdamped “spin” variables are instrumental there for efficient, fast transfer of information through the flock, allowing swift turns in response to threats during which speed is modulated in a well coordinated manner. In the other examples cited above, speed remains nearly constant and the persistently turning tracks of fish or microtubules

reveal some finite, possibly large, memory of the curvature. In this context an Ornstein-Uhlenbeck (OU) process acting on the angular velocity was shown to be a quantitatively valid representation [10,16]. The collective motion of self-propelled particles with such underdamped angular dynamics remains largely unexplored.

In this Letter, we explore minimal models of aligning self-propelled particles with memory similar to that used in Ref. [10] to study the emergence of large-scale vortices in motility assays. Considering both polar (ferromagnetic) and nematic alignment interactions between particles, we show that memory is a crucial ingredient for collective motion giving rise to a wealth of collective states heretofore not observed in the memoryless case. Among the most remarkable features of the rich phase diagram of these minimal models, we provide evidence that global polar order can arise from strictly nematic interactions, taking the form of trains of “Vicsek waves,” i.e., the ubiquitous nonlinear structures well known from models and experimental situations described by the traditional Vicsek model [22,23]. We not only consider OU, but also telegraphic noise (TN) processes, which we show to be more easily amenable to analytic approaches. For these telegraphic noise models, we present a calculation yielding the effective interaction between emerging vortices, and thus a simple explanation of why these structures form hexagonal or square lattices depending on the symmetry of the alignment interaction.

Let us first introduce Vicsek-style models with memory. Point particles with position  $\mathbf{x}_i$  move at unit speed along their heading  $\theta_i(t)$ , i.e.,  $\dot{\mathbf{x}}_i = \mathbf{e}_{\theta_i}$ , where  $\mathbf{e}_{\theta_i}$  is the unit vector along  $\theta_i$ . Headings evolve according to

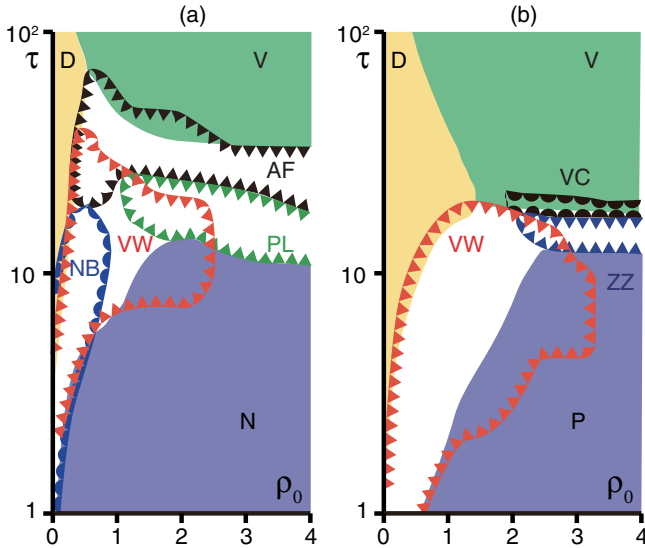


FIG. 1 (color online). Phase diagrams of the models defined by Eqs. (1) and (2). See main text and/or Fig. 2 for definitions of the various phases. (a) Nematic model. (b) Polar model.

$$\frac{d\theta_i}{dt} = \frac{\alpha}{\mathcal{N}_i} \sum_{|x_j - x_i| < 1} \sin[m(\theta_j - \theta_i)] + \omega_i(t), \quad (1)$$

where the sum is over the  $\mathcal{N}_i$  neighbors of  $i$  within unit distance,  $m = 1$  (2) codes for ferromagnetic (nematic) alignment, and  $\omega$  is a zero-mean noise. For uncorrelated white noise, the noise strength and the global density of particles are the two main parameters, and these overdamped models are expected to exhibit a phase diagram similar to that of their discrete-time counterparts [24–26].

Memory is introduced via an Ornstein-Uhlenbeck process for the noise  $\omega$  in Eq. (1), keeping all other compartments of the dynamics overdamped,

$$\frac{d\omega_i}{dt} = -\frac{1}{\tau} \omega_i + \xi_i(t), \quad (2)$$

where  $\xi$  is a Gaussian white noise of variance  $\sigma^2$ . The underdamped models defined by Eqs. (1) and (2) depend on one extra parameter, the memory time  $\tau$ . In the limit of small  $\tau$ , they reduce to their overdamped versions.

In Ref. [10], the nematic version ( $m = 2$ ) of this model was introduced and a preliminary study of its collective regimes was presented in the plane of the mean density  $\rho_0$  and  $\tau$  keeping  $\langle \omega^2 \rangle = \frac{1}{2} \tau \sigma^2$ , the variance of  $\omega$ , fixed [27]. Here, we present a detailed phase diagram of our models in the  $(\rho_0, \tau)$  plane also keeping  $\langle \omega^2 \rangle$  fixed, having checked that its global structure does not vary much with  $\langle \omega^2 \rangle$ . The quantifiers used to define and distinguish the collective states observed and the methodology followed to establish the following phase diagrams are detailed in Ref. [28].

*Nematic model ( $m = 2$ ).*—Its phase diagram is summarized in Fig. 1(a). The three main regions found in Ref. [10] are present. At small enough density, noise always dominates alignment leaving a homogeneous disordered phase (D). At low enough  $\tau$ , homogeneous nematic order emerges (N), while at high enough  $\tau$  one eventually observes a hexagonal lattice of large vortices (V) made with local nematic order [see Fig. 2(a) and Ref. [10]].

Our analysis also revealed the existence of a complex arrangement of other collective states in the area separating these three main regions. Consistent with the overdamped case [26], a coexistence phase made of a dense nematic band (NB) standing in a disordered gas is present between the D and N regions. But there is also a large domain inside which one can observe trains of dense, traveling bands such as those known to occur in overdamped models with ferromagnetic alignment like the original Vicsek model [24,29]. The smectic pattern of Vicsek waves [VW, Fig. 2(c)] is even the only asymptotic state in a subregion of their observation domain. Thus, global polar order arises whereas the interaction is purely nematic [30]. Note that such global order, made of nonlinear structures, is not in contradiction with the theoretical arguments at linear

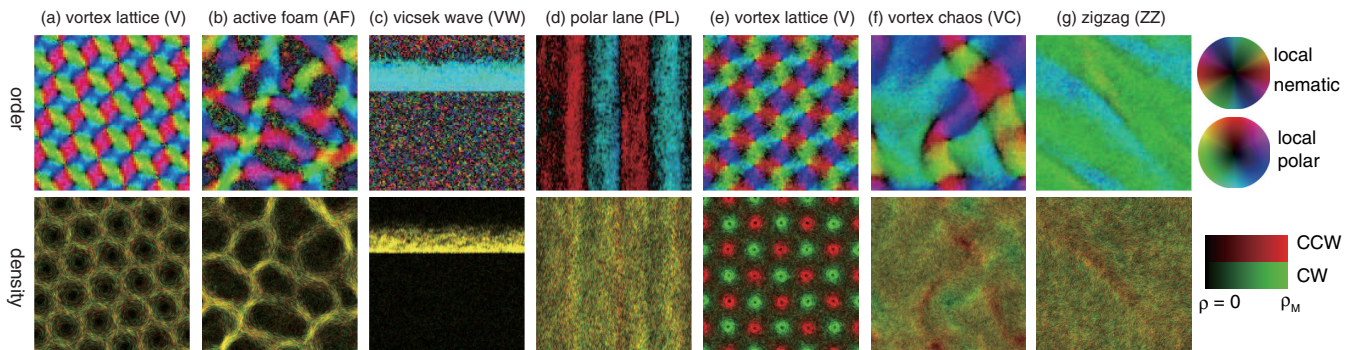


FIG. 2 (color online). Various phases for the nematic (a)–(d) and polar (e)–(g) model. Corresponding movies are available in Ref. [28]. Top: local orientational order [nematic (a),(b); polar (c)–(g)]; color stands for orientation, intensity for modulus. Bottom: superimposed density of clockwise (CW,  $\omega < 0$ , green) and counterclockwise (CCW,  $\omega > 0$ , red) particles. Color maps are on the right, with  $\rho_M = 2$  for (a)–(e), 4 for (f), and 5 for (g). Parameters  $(\rho_0, \tau)$ : (a) (1,100), (b) (1,40), (c) (0.56,10), (d) (1.78,20), (e) (1,100), (f) (4.22, 17.5), and (g) (3.16, 15). Periodic square of linear size 512,  $\alpha = 0.1$ ,  $\langle \omega^2 \rangle^{1/2} = 0.03$  (0.06) for the nematic (polar) model.

level [26,31,32] precluding the emergence of homogeneous polar order in systems with nematic interactions.

The vortex lattice directly melts to the homogeneous disorder state when decreasing  $\tau$  at low densities. For large enough  $\rho_0$ , on the other hand, it becomes a spatiotemporally disordered cellular structure—an “active foam” (AF) [Fig. 2(b)]. This foam is still made of the same nematically ordered streams as the vortex lattice, but they are unstable.

Finally, at large enough densities, increasing  $\tau$ , the homogeneous nematic state becomes transversally unstable. Global nematic order is preserved, but local segregation leads to oppositely going polar lanes of relatively large width [laning region PL in Fig. 1(a), snapshot in Fig. 2(d)]. Laning has been reported in overdamped self-propelled hard rods interacting solely via steric exclusion, and also for elongated “deformable” particles [33,34]. Observed here with pointwise particles, we conclude that neither a long aspect ratio nor even a finite size are necessary. This striped pattern is dynamic: a space-time plot of local polar order across the lanes reveals two sets of lanes (each with lanes in both orientations) moving slowly along this transversal direction, yielding a standing wave pattern (Fig. 3). Whether dynamic laning is also present in rod systems remains to be investigated.

*Polar model ( $m = 1$ ).*—We now describe the phase diagram in the case of ferromagnetic alignment [Fig. 1(b)], which has the same general features as in the nematic case. Three main regions are present: homogeneous disorder (D), homogeneous polar order (P), and vortex lattice (V). This lattice is now a checkerboard arrangement of locally polar clockwise and counterclockwise vortices [Fig. 2(e)]. Again, for short enough memory time  $\tau$ , one recovers, between the D and P phases, the coexistence phase made of a smectic arrangement of Vicsek waves (VW), familiar from the study of the overdamped case. The central region is less complicated than in the nematic case, but nevertheless comprises (at least) two new phases. For  $\rho_0 > 1$ , the vortex lattice gives way to a chaotic phase where vortex cores move, coalesce, vanish,

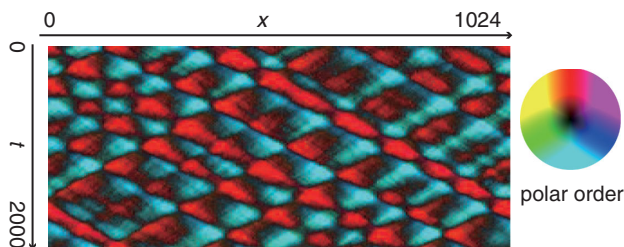


FIG. 3 (color online). Space-time diagram in the laning phase (nematic model). Rectangular domain  $(L_x, L_y) = (1024 \times 256)$  with global nematic order along  $y$  (periodic boundary conditions). Local polar order averaged over  $y$  is represented (color map on right). Parameters:  $(\rho_0, \tau) = (1.33, 20)$  (other parameters as in Fig. 2 for the nematic model).

and form spontaneously [“vortex chaos” (VC), Fig. 2(f)]. Finally, the homogeneous polar order region P is bordered, at large  $\tau$ , by a regime characterized by moving domains inside which polar order is perpendicular to the main direction of motion, so that particles perform “zigzag” trajectories [ZZ region in Fig. 1(b), snapshot in Fig. 2(g)].

Some general comments are in order. For both the nematic and polar models several states are observed to coexist in the central region of parameter space. They can be reached from different initial conditions, and observed for at least the very long time  $T$  that we use here as a criterion for “stability.” Determining which one is dominant, though, is a difficult task beyond the scope of this Letter. However, as already noticed for Vicsek waves in the nematic case, there exists, for each phase, a region where it is the only observed state. Thus, all phases reported here are likely to exist asymptotically. Both models show emergent structures (vortices, lanes) of creatively large scale compared to the unit interaction distance. These scales can be shown to be essentially given by  $\langle \omega^2 \rangle$ .

*Telegraphic noise models.*—Further progress may come from numerical work even more intensive than reported here. Another avenue to ascertain the robustness of our results would be to derive continuous theories for our models. Unfortunately, methods that were proven successful in the overdamped case are difficult to apply here since they rely on the decorrelation of particles between successive interactions. A way out of this conundrum is to replace the Ornstein-Uhlenbeck process (2) by some symmetric Poisson telegraphic noise process  $\omega = \epsilon \omega_0$  in which  $\epsilon = \pm 1$  with a switching probability equal to  $1/\tau$ . Then, indeed, one can consider two subpopulations of particles, clockwise and counterclockwise, exchanging particles at rate  $1/\tau$  via some memoryless Poissonian switching process, similar to that for flipping self-propelled rods in Ref. [20].

We first studied numerically the collective properties of the TN models. Their phase diagrams are qualitatively similar to those presented in Fig. 1 for the OU models (detailed results will be published elsewhere [35, 36]). Almost all phases observed in the OU case are also present with TN. Possibly the only exception is the absence of the active foam regime, which is replaced by a chaotic regime that appears as a superposition of nematic bands and vortices. This points to the robustness of the results presented so far, an indication that Vicsek-style models with memory can probably all be described by some common continuous theory.

Here, we postpone the construction of a full-fledged hydrodynamic theory. Instead, we now show how the structure of the emerging vortex lattice observed at large  $\tau$  and the shape of its region of existence in parameter space can be understood via the calculation of the effective interaction between vortices.

In the vortex region,  $\tau$  is large, which means that one particle typically stays on a circle trajectory for a while.

We take advantage of this to describe the dynamics of the centers  $\mathbf{r}_i$  of these circular trajectories, changing  $\mathbf{x}_i$ , the particle position, to  $\mathbf{r}_i = \mathbf{x}_i + \epsilon_i \omega_0^{-1} (-\sin \theta_i, \cos \theta_i)$ . Differentiating both sides and using Eq. (1) we obtain

$$\dot{\mathbf{r}}_i = \frac{2\epsilon_i \delta(t - t_s)}{\omega_0} \tilde{\mathbf{e}}_{\theta_i} - \frac{\alpha \epsilon_i}{\mathcal{N}_i \omega_0} \sum_{|\mathbf{x}_i - \mathbf{x}_j| < 1} \sin[m(\theta_j - \theta_i)] \mathbf{e}_{\theta_i}, \quad (3)$$

where  $\tilde{\mathbf{e}}_{\theta_i} = \mathbf{e}_{\theta_i - (\pi/2)}$  and  $t_s$  is the time when  $\epsilon_i$  switches between  $\pm 1$ . Assuming that  $\mathcal{N}_i = 1$ , we describe the ensemble behavior of Eqs. (3) by the number densities of clockwise or counterclockwise particles  $f_{\pm}(\mathbf{r}, \theta)$  satisfying the equations (see Ref. [20])

$$\frac{\partial f_{\pm}(\mathbf{r}, \theta)}{\partial t} = \pm \frac{\partial}{\partial \mathbf{r}} \cdot \mathbf{e}_{\theta} f_{\pm}(\mathbf{r}, \theta) \frac{U_{\pm}}{\omega_0} - \frac{\partial}{\partial \theta} f_{\pm}(\mathbf{r}, \theta) (\pm \omega_0 + U_{\pm}) + \frac{f_{\mp}(\mathbf{r} \pm D \tilde{\mathbf{e}}_{\theta}, \theta) - f_{\pm}(\mathbf{r}, \theta)}{\tau} \quad (4)$$

with the collective rotation rates

$$U_{\pm} = \alpha \sum_{\mu=-1,1} \int d\xi \int_{-\pi}^{\pi} d\phi \chi(\mathbf{x}_{\xi, \phi}^{\mu}, \mathbf{x}_{\mathbf{r}, \theta}^{\pm 1}) f_{\mu}(\xi, \phi) \sin[m(\phi - \theta)].$$

Here,  $\chi(\mathbf{x}', \mathbf{x})$  is 1 (0) when  $|\mathbf{x}' - \mathbf{x}| < (\geq) 1$ ,  $\mathbf{x}_{\mathbf{r}, \theta}^{\epsilon} = \mathbf{r} + \epsilon/\omega_0 \tilde{\mathbf{e}}_{\theta}$ , and  $D = 2/\omega_0$ . To simplify Eqs. (4), we average over the rotation period and assume the distributions to be almost uniform in  $\theta$  (an assumption that is valid below the onset of the ordered phase when  $\theta$  changes little during one collision [37]). Defining  $F_{\pm}(\mathbf{r}) = \int_0^{2\pi} f_{\pm}(\mathbf{r}, \theta) d\theta / 2\pi$  we obtain

$$\frac{\partial F_{\pm}}{\partial t} = -D\alpha \frac{\partial}{\partial \mathbf{r}} \cdot F_{\pm}(\mathbf{r}) \int d\xi \mathbf{K}(\mathbf{r} - \xi) [F_{\pm}(\xi) + (-1)^m F_{\mp}(\xi)] + \frac{1}{\tau} \left\{ \frac{1}{2\pi} \int_0^{2\pi} d\theta F_{\mp}(\mathbf{r} + D\mathbf{e}_{\theta}) - F_{\pm}(\mathbf{r}) \right\}, \quad (5)$$

where the radial interaction kernel

$$\mathbf{K}(\mathbf{r}) = - \int_{-\pi}^{\pi} d\theta \int_{-\pi}^{\pi} d\phi \chi(\mathbf{x}_{0, \phi}^1, \mathbf{x}_{\mathbf{r}, \theta}^1) \sin[m(\phi - \theta)] \frac{\mathbf{e}_{\theta}}{4\pi} \quad (6)$$

is shown in Figs. 4(a) and 4(b) (see Ref. [28] for details). The interaction is short range:  $\mathbf{K}(\mathbf{r}) = 0$  for  $|\mathbf{r}| > D + 1$ . In the polar case ( $m = 1$ ), it is attractive (repulsive) between vortices rotating in the same (opposite) direction. In the nematic case ( $m = 2$ ), the interaction has a short-range attractive part and a medium range repulsive part.

We examined the stability of a homogeneous state  $F_+ = F_- = \rho_0/2$ . Linearizing Eqs. (5), we obtain after the Fourier transform

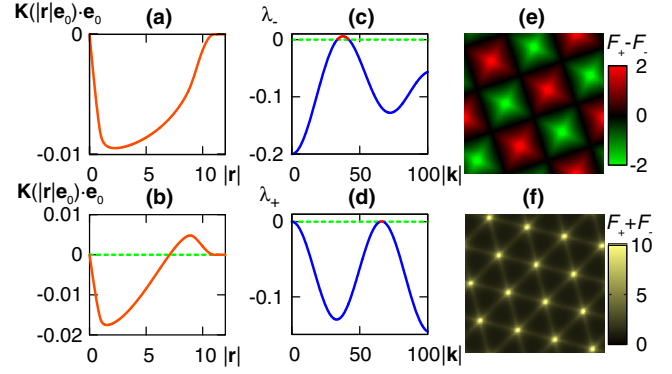


FIG. 4 (color online). Continuous description for vortex lattice formation. Top (bottom) row: polar (nematic) model. (a),(b) Effective interaction. (c),(d) Dispersion relation (eigenvalue for  $F_+ - F_-$ ,  $F_+ + F_-$ ). (e),(f) Steady states when  $\rho_0\tau$  is larger than the critical value. (e) shows  $F_+ - F_-$ , and (f) shows  $F_+ + F_-$ . Periodic square of linear size 40,  $D = 10$ ,  $\alpha = 0.05$ , and  $\rho_0 = 0.02$ . In the polar (nematic) interaction case,  $\rho_0\tau = 0.2$  (0.17).

$$\frac{dF_{\pm}^{\mathbf{k}}}{dt} = \left( (-1)^{m+1} \pi D \alpha |\mathbf{k}| K^{|\mathbf{k}|} \rho_0 + \frac{J_0(|\mathbf{k}|D)}{\tau} \right) F_{\mp}^{\mathbf{k}} - \left( \pi D \alpha |\mathbf{k}| K^{|\mathbf{k}|} \rho_0 + \frac{1}{\tau} \right) F_{\pm}^{\mathbf{k}}. \quad (7)$$

$J_n$  is the  $n$ th Bessel function of the first kind, and  $K^{|\mathbf{k}|} = \int_0^{D+1} dr J_1(|\mathbf{k}|r) r \mathbf{e}_0 \cdot \mathbf{K}(r \mathbf{e}_0)$ . Examining the eigenvalues of Eq. (7), we find that the homogeneous state becomes unstable when  $\rho_0\tau > c_{\min}$ ,  $c_{\min} = \min_{|\mathbf{k}|} [((-1)^m J_0(|\mathbf{k}|D) - 1) / (2\pi D \alpha |\mathbf{k}| K^{|\mathbf{k}|})]$  [Figs. 4(c) and 4(d)]. In the nematic case, due to the conservation of particles,  $F_+^0 + F_-^0$  is neutral, see Fig. 4(d). The corresponding amplitude equation is the conserved Swift-Hohenberg equation [38]. It yields hexagonal lattices, consistent with our findings. In the polar case, the unstable mode  $F_+ - F_-$  would yield the conventional Swift-Hohenberg equation with cubic nonlinearity. But conservation of particles implies that the unstable mode couples to the neutral mode  $F_+ + F_-$  at  $|\mathbf{k}| = 0$ . A square lattice is then expected [39], again in agreement with our results. Numerical integration of Eqs. (5) confirms that for  $\rho_0\tau > c_{\min}$  the correct periodic lattice emerges, Figs. 4(e) and 4(f). The instability condition  $\rho_0\tau > c_{\min}$  is in semi-quantitative agreement with simulations of the particle models with TN.

To summarize, we have shown that memory, in the form of underdamped angular dynamics, is a crucial ingredient for the collective properties of self-propelled particles. Our Vicsek-style models exhibit a prominent vortex lattice phase at high density and large memory. With nematic alignment a hexagonal lattice emerges, but polar interactions lead to a checkerboard square lattice of alternating vortices, a fact explained by the calculation. We have also shown the emergence of a number of collective states for

moderate memory times. In particular, we observed the emergence, out of purely nematic interactions, of global, long-range, polar order made of Vicsek waves. We also reported that nematic interactions can give rise to a system of traveling polar lanes. Such laning configurations have been reported for overdamped self-propelled elongated objects interacting via steric exclusion [33]. Thus, repeated collisions between these rods seem to amount to some effective memory. Laning may in fact be best characterized this way, and not necessarily by the aspect ratio of particles.

Even though smooth trajectories with persistent curvature are observed for birds, swimmers, etc., the studied models are probably most suited for self-organization phenomena in *in vitro* mixtures of biofilaments and motor proteins such as motility assays. Nematic vortices were already reported in Ref. [10], and Vicsek wavelike patterns in Ref. [9]. We are confident that some of the other phases reported here are also present in such systems.

We thank the Max Planck Institute for the Physics of Complex Systems, Dresden, for providing the framework of the Advanced Study Group “Statistical Physics of Collective Motion” within which part of this work was conducted. K. H. N. was supported by a Grant-in-Aid for Scientific Research on Innovative Areas “Fluctuation & Structure” (No. 26103505), and a JSPS fellowship for young scientists (No. 23-1819). Y. S. was supported by a Grant-in-Aid for Young Scientists B (No. 24740287), and the Cooperative Research Program of “Network Joint Research Center for Materials and Devices.” I. S. A. was supported by the U.S. Department of Energy, Office of Science, Basic Energy Sciences, Materials Science and Engineering Division.

- 
- [1] A. Kudrolli, G. Lumay, D. Volfson, and L. S. Tsimring, *Phys. Rev. Lett.* **100**, 058001 (2008).  
 [2] V. Narayan, S. Ramaswamy, and N. Menon, *Science* **317**, 105 (2007).  
 [3] I. S. Aranson, D. Volfson, and L. S. Tsimring, *Phys. Rev. E* **75**, 051301 (2007).  
 [4] J. Deseigne, O. Dauchot, and H. Chaté, *Phys. Rev. Lett.* **105**, 098001 (2010); J. Deseigne, S. Léonard, O. Dauchot, and H. Chaté, *Soft Matter* **8**, 5629 (2012).  
 [5] N. Kumar, H. Soni, S. Ramaswamy, and A. K. Sood, *Nat. Commun.* **5**, 4688 (2014).  
 [6] J. Palacci, S. Sacanna, A. P. Steinberg, D. J. Pine, and P. M. Chaikin, *Science* **339**, 936 (2013).  
 [7] I. Theurkauff, C. Cottin-Bizonne, J. Palacci, C. Ybert, and L. Bocquet, *Phys. Rev. Lett.* **108**, 268303 (2012).  
 [8] A. Bricard, J.-B. Caussin, N. Desreumaux, O. Dauchot, and D. Bartolo, *Nature (London)* **503**, 95 (2013).  
 [9] V. Schaller, C. Weber, C. Semmrich, E. Frey, and A. R. Bausch, *Nature (London)* **467**, 73 (2010); *Soft Matter* **7**, 3213 (2011); *Proc. Natl. Acad. Sci. U.S.A.* **108**, 19183 (2011).

- [10] Y. Sumino, K. H. Nagai, Y. Shitaka, D. Tanaka, K. Yoshikawa, H. Chaté, and K. Oiwa, *Nature (London)* **483**, 448 (2012).  
 [11] T. Sanchez, D. T. N. Chen, S. J. DeCamp, M. Heymann, and Z. Dogic, *Nature (London)* **491**, 431 (2012).  
 [12] F. Peruani, J. Staruß, V. Jakovljevic, L. Søgaard-Andersen, A. Deutsch, and M. Bär, *Phys. Rev. Lett.* **108**, 098102 (2012).  
 [13] H. H. Wensink, J. Dunkel, S. Heidenreich, K. Drescher, R. E. Goldstein, H. Lowen, and J. M. Yeomans, *Proc. Natl. Acad. Sci. U.S.A.* **109**, 14308 (2012).  
 [14] A. Attanasi *et al.*, *Phys. Rev. Lett.* **113**, 238102 (2014).  
 [15] H. Hildenbrandt, C. Carere, and C. K. Hemelrijk, *Behav. Ecol.* **21**, 1349 (2010); D. J. G. Pearce, A. M. Miller, G. Rowlands, and M. S. Turner, *Proc. Natl. Acad. Sci. U.S.A.* **111**, 10422 (2014); A. Cavagna *et al.*, *J. Stat. Phys.* **158**, 601 (2015).  
 [16] J. Gautrais, C. Jost, M. Soria, A. Campo, S. Motsch, R. Fournier, S. Blanco, and G. Theraulaz, *J. Math. Biol.* **58**, 429 (2009); *PLoS Comput. Biol.* **8**, e1002678 (2012);  
 [17] I. Karamouzas, B. Skinner, and S. J. Guy, *Phys. Rev. Lett.* **113**, 238701 (2014).  
 [18] P. Romanczuk, M. Bär, W. Ebeling, B. Lindner, and L. Schimansky-Geier, *Eur. Phys. J. Spec. Top.* **202**, 1 (2012).  
 [19] W. F. Paxton, K. C. Kistler, C. C. Olmeda, A. Sen, S. K. St. Angelo, Y. Cao, T. E. Mallouk, P. E. Lammert, and V. H. Crespi, *J. Am. Chem. Soc.* **126**, 13424 (2004).  
 [20] D. Takagi, A. B. Braunschweig, J. Zhang, and M. J. Shelley, *Phys. Rev. Lett.* **110**, 038301 (2013).  
 [21] A. Attanasi *et al.*, *Nat. Phys.* **10**, 691 (2014); A. Cavagna *et al.*, [arXiv:1410.2868](https://arxiv.org/abs/1410.2868).  
 [22] G. Grégoire and H. Chaté, *Phys. Rev. Lett.* **92**, 025702 (2004).  
 [23] T. Vicsek, A. Czirok, E. Ben-Jacob, I. Cohen, and O. Shochet, *Phys. Rev. Lett.* **75**, 1226 (1995).  
 [24] H. Chaté, F. Ginelli, G. Grégoire, and F. Raynaud, *Phys. Rev. E* **77**, 046113 (2008); A. P. Solon, H. Chaté, and J. Tailleur, *Phys. Rev. Lett.* **114**, 068101 (2015).  
 [25] H. Chaté, F. Ginelli, and R. Montagne, *Phys. Rev. Lett.* **96**, 180602 (2006); S. Ngo, A. Peshkov, I. S. Aranson, E. Bertin, F. Ginelli, and H. Chaté, *Phys. Rev. Lett.* **113**, 038302 (2014).  
 [26] F. Ginelli, F. Peruani, M. Bär, and H. Chaté, *Phys. Rev. Lett.* **104**, 184502 (2010); A. Peshkov, I. S. Aranson, E. Bertin, H. Chaté, and F. Ginelli, *Phys. Rev. Lett.* **109**, 268701 (2012).  
 [27] This choice guarantees that for large  $\tau$  the size of vortices, which is governed by  $\langle \omega^2 \rangle$ , remains roughly constant.  
 [28] See Supplemental Material at <http://link.aps.org/supplemental/10.1103/PhysRevLett.114.168001> for movies and details of the calculation of the effective interaction between vortices.  
 [29] The Vicsek model bands first reported in Ref. [23] have since been observed in many other models. See, e.g., S. Mishra, A. Baskaran, and M. C. Marchetti, *Phys. Rev. E* **81**, 061916 (2010); C. A. Weber, T. Hanke, J. Deseigne, S. Léonard, O. Dauchot, E. Frey, and H. Chaté, *Phys. Rev. Lett.* **110**, 208001 (2013); P. Romanczuk and L. Schimansky-Geier, *Interface Focus* **2**, 746 (2012).

- [30] When starting from random initial conditions, counter-propagating bands are typically observed. After a long transient, one direction eventually wins, leaving a wave train moving in the same direction—global polar order.
- [31] C. W. Harvey, M. Alber, L. S. Tsimring, and I. S. Aranson, *New J. Phys.* **15**, 035029 (2013).
- [32] A. Baskaran and M. C. Marchetti, *Phys. Rev. E* **77**, 011920 (2008); *Phys. Rev. Lett.* **101**, 268101 (2008).
- [33] H. H. Wensink and H. Löwen, *J. Phys. Condens. Matter* **24**, 464130 (2012); S. R. McCandlish, A. Baskaran, and M. F. Hagan, *Soft Matter* **8**, 2527 (2012); A. M. Menzel, *J. Phys. Condens. Matter* **25**, 505103 (2013); T. Gao, R. Blackwell, M. A. Glaser, M. D. Betterton, and M. J. Shelley, *Phys. Rev. Lett.* **114**, 048101 (2015); H.-S. Kuan *et al.*, arXiv:1407.4842.
- [34] A. M. Menzel and T. Ohta, *Europhys. Lett.* **99**, 58001 (2012).
- [35] Y. Sumino *et al.* (to be published).
- [36] Note that it was shown in B. C. Bag, K. G. Petrosyan, and C. K. Hu, *Phys. Rev. E* **76**, 056210 (2007) and R. Tönjes, *Phys. Rev. E* **81**, 055201(R) (2010) that OU-correlated noise facilitates synchronization in the Kuramoto model, which is consistent with our findings.
- [37] I. S. Aranson and L. S. Tsimring, *Phys. Rev. E* **71**, 050901 (2005); **74**, 031915 (2006).
- [38] K. R. Elder, M. Katakowski, M. Haataja, and M. Grant, *Phys. Rev. Lett.* **88**, 245701 (2002).
- [39] L. S. Tsimring and I. S. Aranson, *Phys. Rev. Lett.* **79**, 213 (1997).